AD-787 043

TORSIONAL SHEAR MEASUREMENTS OF THE FRICTIONAL PROPERTIES OF WESTERLY GRANITE

Roland J. Christensen, et al

Utah University

Prepared for:

Defense Nuclear Agency

31 May 1974

DISTRIBUTED BY:

NTIS

National Technical Information Service
U. S. DEPARTMENT OF COMMERCE
5285 Port Royal Road, Springfield Va. 22151

Unclassified

SECURITY CLASSIFICATION OF THIS PAGE (When Data Entered)

REPORT DOCUMENTATION PAGE

READ INSTRUCTIONS BEFORE COMPLETING FORM

1. REPORT NUMBER: DNA 3359F

2. GOVT ACCESSION NO.:

3. RECIPIENT'S CATALOG NUMBER: AD-787 043

4. TITLE (and Subtitle): Torsional Shear Measurements of the Frictional Properties of Westerly Granite

5. TYPE OF REPORT & PERIOD COVERED: Final Report, 1 Sept. 1972 - 31 July 1974

6. PERFORMING ORG. REPORT NUMBER: UTEC ME 73-055 or TR 73-64

7. AUTHOR(s):
Roland J. Christensen
Stephen R. Swanson
Wayne S. Brown

8. CONTRACT OR GRANT NUMBER(s): DNA001-73-C-0034

9. PERFORMING ORGANIZATION NAME AND ADDRESS:
University of Utah
Dept. Mechanical Engineering
Salt Lake City, Utah 84112

10. PROGRAM ELEMENT, PROJECT, TASK AREA & WORK UNIT NUMBERS:
Y99QAXS
B047
55

11. CONTROLLING OFFICE NAME AND ADDRESS:
Headquarters
Defense Nuclear Agency
Washington, D.C. 20305

12. REPORT DATE: 31 May 1974

13. NUMBER OF PAGES: 49

14. MONITORING AGENCY NAME & ADDRESS (if different from Controlling Office):

15. SECURITY CLASS (of this report): Unclassified

15a. DECLASSIFICATION/DOWNGRADING SCHEDULE:

16. DISTRIBUTION STATEMENT (of this Report):

Approved for public release; distribution unlimited.

17. DISTRIBUTION STATEMENT (of the abstract entered in Block 20, if different from Report):

18. SUPPLEMENTARY NOTES

This work was sponsored by the Defense Nuclear Agency under Subtask Y99QAXSB047-55.

19. KEY WORDS (Continue on reverse side if necessary and identify by block number)

shear stress	Westerly granite
shear strain	friction
strength	coefficient-of-friction
deformation	load
	torsion

D D C
RECEIVED
OCT 16 1974
C

20. ABSTRACT (Continue on reverse side if necessary and identify by block number)

(see reverse side)

Reproduced by
NATIONAL TECHNICAL INFORMATION SERVICE
U S Department of Commerce
Springfield VA 22151

DD FORM 1 JAN 73 1473 EDITION OF 1 NOV 65 IS OBSOLETE

Unclassified

SECURITY CLASSIFICATION OF THIS PAGE (When Data Entered)

Item 20. Abstract

Laboratory tests were conducted to measure the frictional properties of Westerly granite with ground surfaces. Torsional shear tests were conducted under confining pressure and axial stress. A strong dependency of the coefficient of friction on the state of stress was established, in addition to the usual dependency on normal stress. A three decade increase in the rate of shearing deformation showed no increase in coefficient of friction.

TABLE OF CONTENTS

LIST OF ILLUSTRATIONS ii

LIST OF TABLES iii

INTRODUCTION 1

EXPERIMENTS 7

EXPERIMENTAL RESULTS 17

DISCUSSION OF RESULTS 31

SUMMARY AND CONCLUSIONS 43

ACKNOWLEDGMENT 44

REFERENCES 45

DISTRIBUTION LIST 47

LIST OF ILLUSTRATIONS

Figure 1.	Direct shear, triaxial, and torsional type specimens used for measuring frictional properties.	2
Figure 2.	Torsional test apparatus.	8
Figure 3.	Overall schematic of apparatus.	9
Figure 4.	Schematic of pressure vessel.	10
Figure 5.	Schematic showing method of getting instrumentation leads out of the pressure vessel.	11
Figure 6.	Torsional joint specimen, load cell, and cantilever displacement gages.	13
Figure 7.	Typical joint surface before and after testing.	18
Figure 8.	Effect of normal stress on maximum residual frictional shear stress for hollow cylinders of Westerly granite with ground surfaces.	19
Figure 9.	Effect of normal stress on residual coefficient of friction for Westerly granite with ground surfaces.	22
Figure 10.	Effect of tangential joint displacement on shear stress for Westerly granite.	23
Figure 11.	Effect of tangential joint displacement on shear stress for Westerly granite.	24
Figure 12.	Effect of tangential joint displacement on shear stress for Westerly granite.	25
Figure 13.	Effect of deformation rate on maximum shear stress for Westerly granite.	27
Figure 14.	Shear stress versus tangential joint displacement for Westerly granite with ground friction surface at medium deformation rate.	28
Figure 15.	Oscilloscope traces for 1 in/sec deformation rate tests.	29
Figure 16.	Failure locus for Westerly granite.	33
Figure 17.	Comparison of failure envelope for intact rock and stress at residual slip of jointed specimens.	34
Figure 18.	Illustration of calculation of fracture coefficient for jointed specimens.	35

LIST OF ILLUSTRATIONS (continued)

Figure 19. Effect of stress state and normal stress on residual friction for Westerly granite. 36

Figure 20. Comparison of present data with Byerlee's data for Westerly granite. 38

Figure 21. Comparison of present data and theory with Byerlee's data of Westerly granite. 39

Figure 22. Predicted effect of joint angle in triaxial jointed specimen. 41

LIST OF TABLES

Table I. Residual Friction Test Data 20

Table II. Medium Deformation Rate Residual Friction Test Data 30

INTRODUCTION

This report presents the results of a laboratory investigation of the strength and deformation of jointed Westerly granite torsion specimens with ground surfaces. The use of torsion specimens to investigate the properties of rock joints has been discussed by Jaeger and Cook[1] but its implementation appears to be unique to the present investigation. The advantages of the torsional test specimen and test apparatus are that the same surfaces are in contact throughout the experiment and the effects of large amounts of sliding on the surfaces may be studied.

The laboratory study of the motion of rock joints under stress is a necessary prerequisite to determine the motion of jointed rock in field problems such as earthquakes and stress wave loadings. A knowledge of the physical properties of joints, intact rock, and the interaction of the two for various geometries is basic to solving these problems. Due to the large number of variables involved in rock joint response, including rock type, surface roughness, size of joint, joint spacing, joint gouge or filler material, rate of loading and state of stress, a combination of field tests, laboratory studies, and numerical analysis may be required to establish working solutions to the problem of defining the motion of jointed rock masses. The present study is limited to the response of Westerly granite with ground surfaces to different states of stress and rate of loading.

Properties of joints have been studied in many experimental investigations. In general, these studies can be divided into three major categories: direct shear tests,[2-10] triaxial tests,[1,9-13] and in situ tests.[3] An illustration of the specimen configurations used for the first two types is shown in Figure 1.[1] The direct shear tests are often limited to low normal stress (usually less than 1000 psi). At these low stresses it is observed that the coefficient of friction is a function of surface roughness.[2,5,7] As the surface roughness increases the joint becomes more interlocked, increasing the coefficient of friction. No general trend for changes in the coefficient of friction with changes in normal stress in all rocks can be established. For a specific rock the coefficient of friction may increase,[2-3] decrease,[2,3,6,7,8] or stay essentially constant[2,3,10] with increasing normal stress.

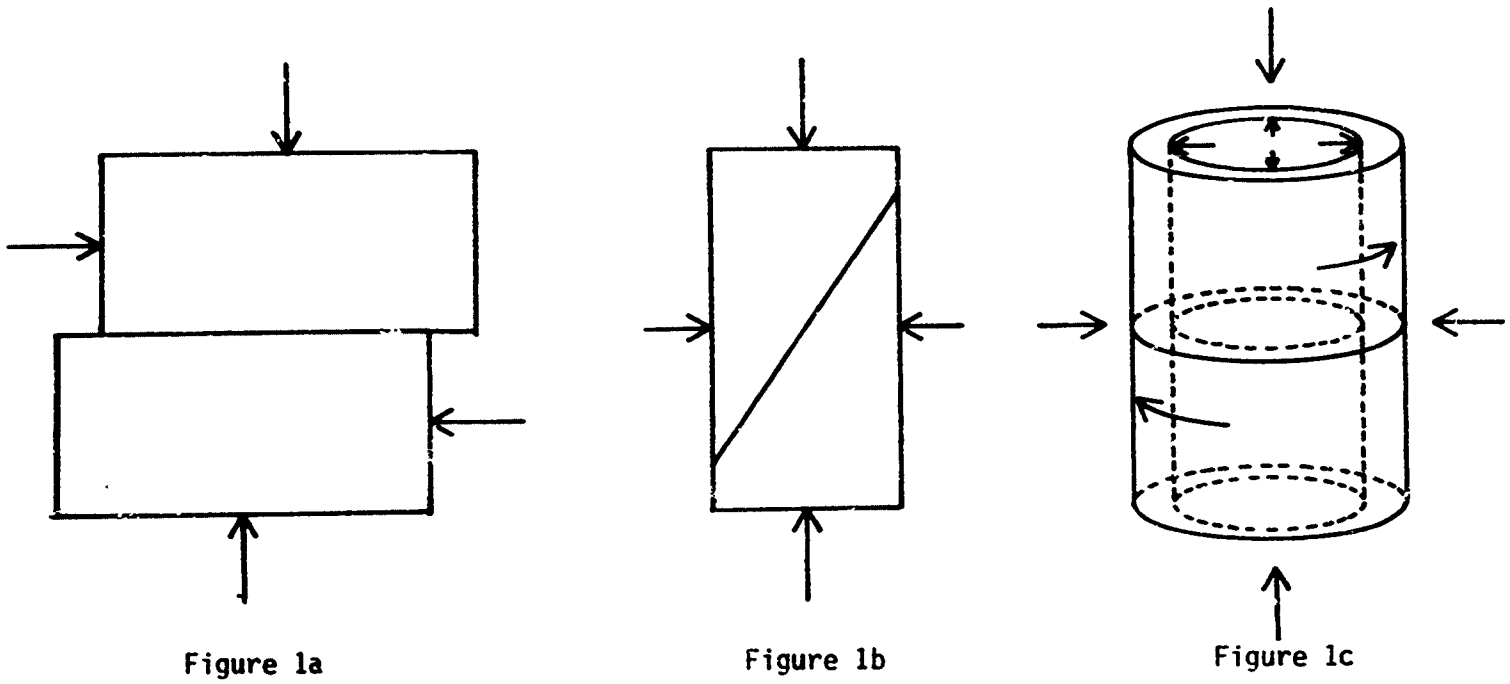

Figure 1. Direct shear, triaxial, and torsional type specimens used for measuring frictional properties.

In the triaxial tests, the normal stresses are generally much higher than in direct shear tests. The stresses in the specimen can be resolved into shear and normal components along the joint to determine the coefficient of friction. At higher normal stresses the surface roughness is less important inasmuch as the rough joint becomes smoother by asperities being sheared off and the smooth joint becomes rougher as slip takes place.[11] Also for both types of roughness, surface gouge or fill material is generated which modifies the effect of the initial roughness. Thus, the coefficient of friction tends to the same value for all surfaces but the relative shearing displacement characteristics may be different. It has been noted that the coefficient of friction often decreases with increasing normal stress in the triaxial test.[1,10-13] Good correlation between direct shear and triaxial tests of joints has been obtained, however, by Jaeger and Rosengren,[10] for normal stresses in the range of 500 to 5,000 psi.

Although tests have not been carried out on the same rock and surface condition, coefficients of friction obtained in triaxial tests at normal stresses of approximately 30 ksi and higher appear to be decreasing with increasing normal stress, and yet are higher than coefficients of friction measured with normal stresses in the range of 1,000 psi.[10-11] This suggests that either μ (the coefficient of friction) increases and then decreases with normal stress or else the results are not compatible due to changes in the experimental conditions.

For many rock types stick-slip or jerky motion is observed in the tangential joint displacement in both triaxial and direct shear type tests.[1,2,5,9,11] Stick-slip is very pronounced in some rocks causing stress drops of up to two-thirds the applied load depending on the stiffness of the loading machine. This behavior has been suggested as the source mechanism for earthquakes.[1,14,15] It is believed that as the loading rate is increased that stick-slip is reduced.[15-16]

The mechanism of dry friction in metals has been postulated by Bowden and Tabor[17] and many others to consist of the welding together of asperity tips under the very large local pressures. Byerlee[7] has concluded, however, that friction in rocks is due to the interaction of brittle asperity tips rather than plastic flow. Evidence in favor of the brittle

fracture theory has been indirect, such as microscopic examination of gouge particles. The presumed very large local stresses at the points of contact in frictional sliding make it difficult to extrapolate directly from the usual laboratory studies of rock brittle fracture and plastic flow.

Dieterich[8] has shown that the time duration of the normal stress application has an effect on the coefficient of friction in rock; increasing the time that the normal stress is applied increases the coefficient of friction. Rabinowicz[18] and Dokos[19] have shown a similar effect in metals and presumably this may be related to the stick-slip phenomenon.

Although the previous investigations have contributed much to the present knowledge of rock joint behavior, a number of important areas are still not well understood. For example, clarifications are needed on the effect of normal stress on the coefficient of friction. Also, the effect of the general state of stress in addition to the normal and shear stress on the joint has not been well investigated. The present study was designed to investigate both of the above problems, and in addition provide data on rate of loading effects.

To accomplish these objectives tests were performed on jointed tubular rock specimens using a torsional shear apparatus. Since this arrangement has not been used previously, a discussion will be given here of the various features as contrasted with direct shear and triaxial compression experiments.

The direct shear apparatus is commonly used for frictional studies since it permits relatively large surfaces to be subjected to relatively large displacements. It suffers from the limitation that for practical reasons the maximum normal stress is usually not higher than 1,000 psi. Also, the state of stress is limited to a normal and a shear stress across the joint. Additionally Kutter[20] has indicated that in such a test the shear stress cannot be uniform across the joint. Since the joint edges are stress free, the shear must be zero at these points and then build up to a maximum in the interior of the specimen.

The triaxial compression test is often employed to obtain joint properties at high normal stresses. The specimen used is commonly much smaller than the direct shear specimen (the shear area is usually on the order of 1/2 to 5 square inches). Since the alignment of the specimen is

disturbed when it is displaced, the joint displacement is limited. The state of stress at the joint consists of a lateral stress equal to the confining pressure, a normal stress equal to the confining pressure plus a component that is related to the axial stress and the joint angle. The state of stress can be varied a limited amount by using different joint angles.

The torsional jointed specimen (illustrated in Figure 1) has some specific advantages. The normal and shear stresses on the joint can be independently controlled, thus facilitating the study of the interaction between normal and shear loadings. Also the state of stress can be varied by changing the superimposed axial loading and confining pressure. The amount of joint slip displacement is theoretically unlimited and in practice can be quite large.

The disadvantages of the torsional joint specimen as used in the present study are twofold; first the joint area is no larger than used in high pressure triaxial joint studies, and second, a non-uniform stress may occur over the joint area. This latter effect will be discussed in more detail in the experimental section.

EXPERIMENTS

Description of Experimental Apparatus

An overall view of the torsion test apparatus is shown in Figure 2. The apparatus consists of a hydraulic ram capable of 220,000 lb axial force, a hydraulic rotary actuator capable of applying a torque of 60,000 in-lb, and a pressure vessel to allow confining pressure up to 50,000 psi to be applied to the sample. All stress conditions can be applied independently. The hydraulic ram, rotary actuator, and the pressure intensifier were all servo-controlled so that each component of the system could be controlled by either a displacement or load type feedback. The servo valves were limited to a flow rate of 15 gallons per minute which made it possible to run tests at strain rates up to 1/sec in both axial and torsional modes.

A schematic of the overall view of the apparatus is shown in Figure 3. The rotary actuator is mounted on a steel plate at the bottom. The next major part of the apparatus is a connection that links the rotary actuator to the hydraulic ram. This coupler must transmit the torque and allow for the axial displacement for the hydraulic cylinder. A cylinder with six keys and key ways was used to accomplish this. Above this is the hydraulic ram with double-ended piston designed to rotate so the torque could be transmitted through it. Finally, the pressure vessel is situated on top in a manner that allows samples to be easily inserted for testing.

The pressure vessel assembly was made from 4340 alloy steel with a mild steel safety ring press fit on the outside. A schematic is shown in Figure 4. Standard O-ring seals were used to seal both ends of the pressure vessel. Figure 4 also shows the arrangement of the sample, load cell, base plug and piston when this sample is ready for testing. As can be seen the torque and axial load are transmitted from the piston of the hydraulic ram to the piston going into the pressure vessel. The base plug is kept from rotating by the top plate which is attached to the main frame by means of the bolts and the safety ring.

Figure 5 shows the scheme used to get electrical leads for instrumentation out of the pressure vessel. A stainless steel cone lined with a nylon insert (to both insulate the cone from the vessel and form a seal) has proven satisfactory in previous studies[21] and was found to be successful in this program.

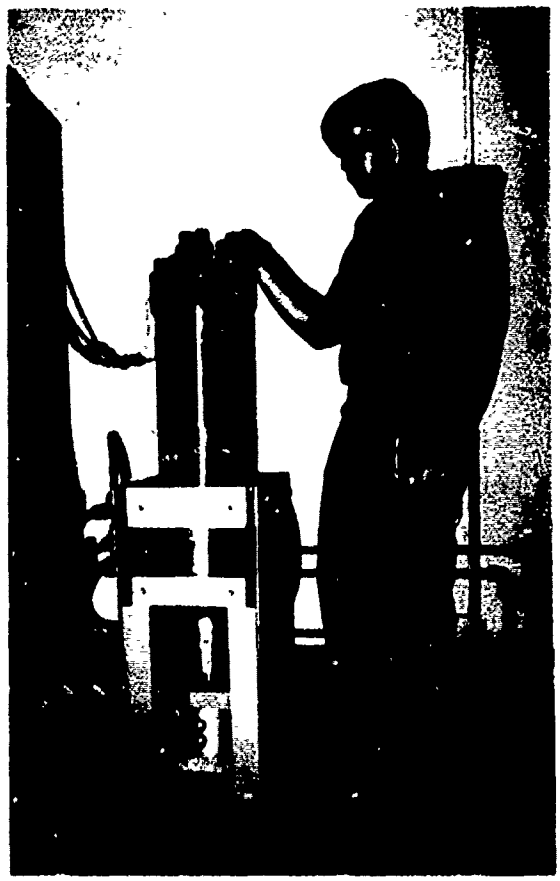

Figure 2. Torsional test apparatus.

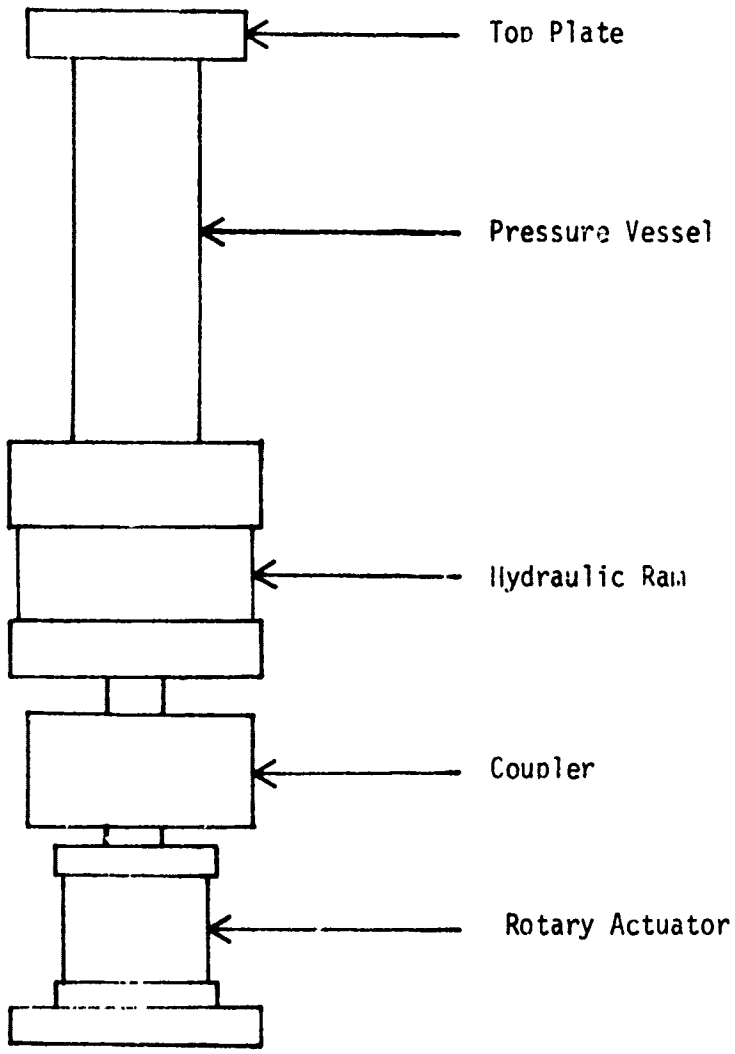

Figure [illegible]. Overall schematic of a [illegible].

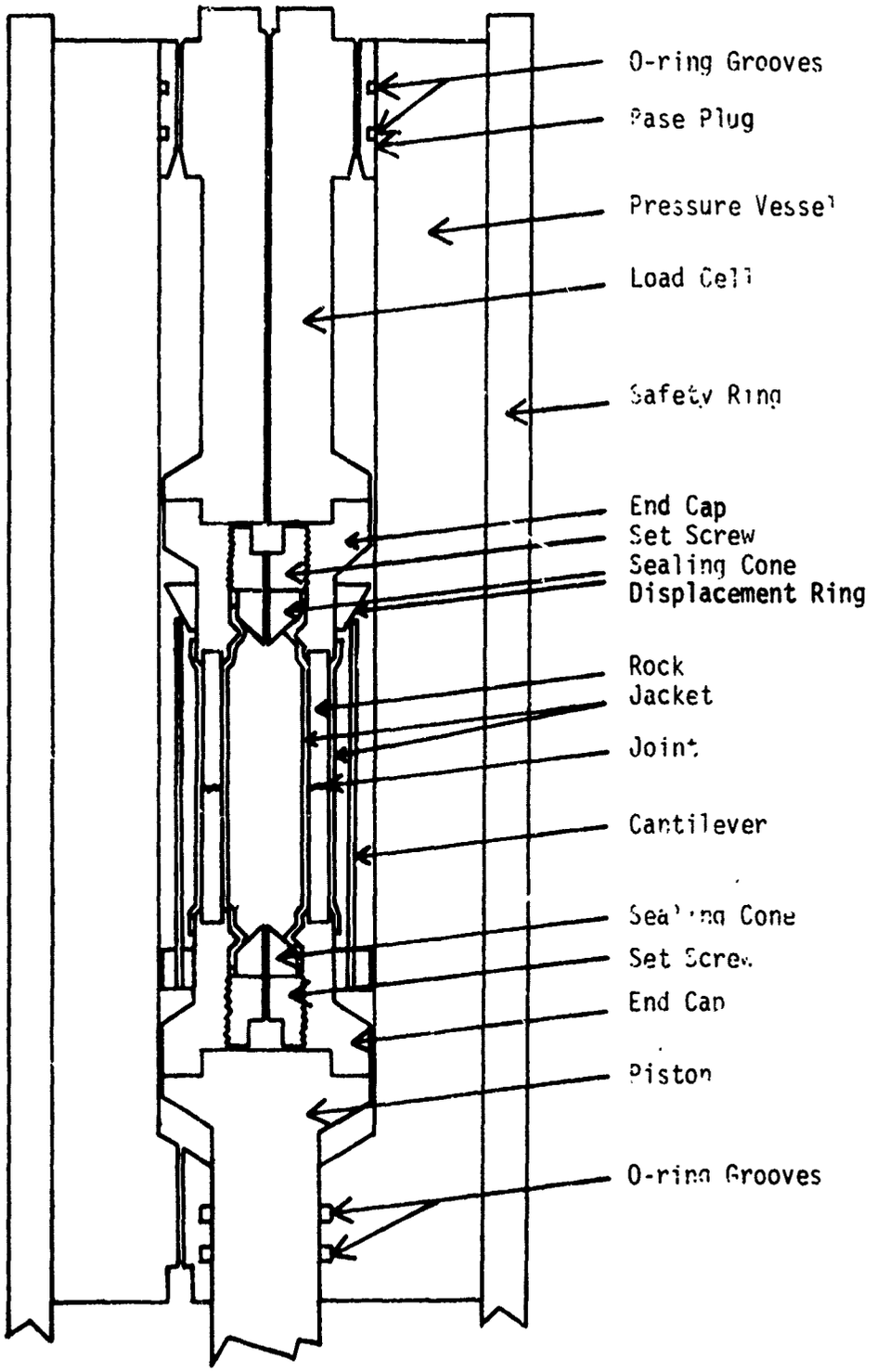

Figure 4. Schematic of Pressure Vessel.

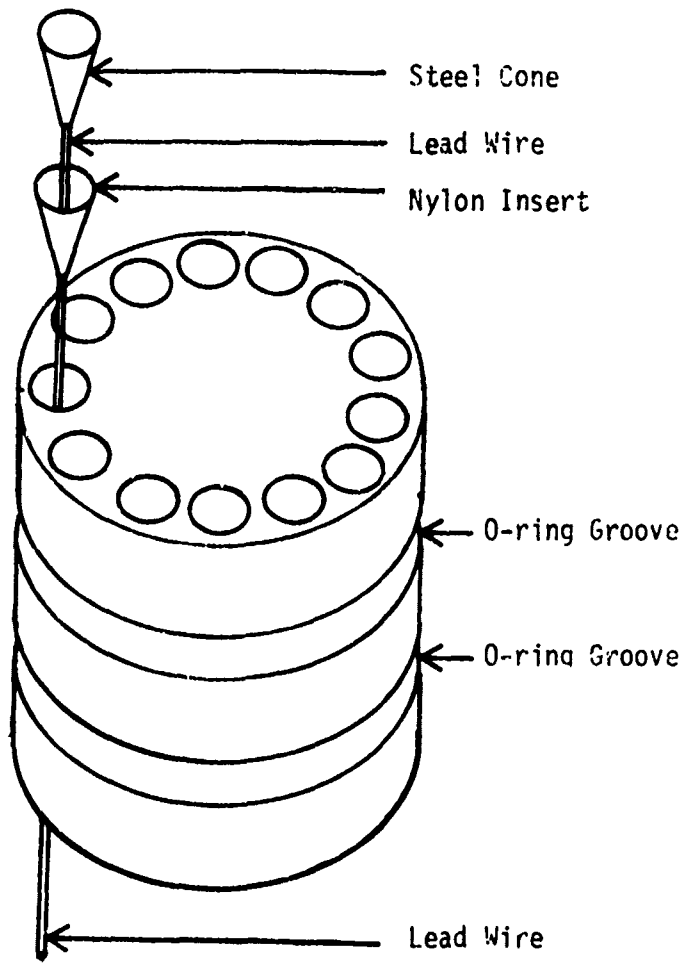

Figure 5. Schematic showing method of getting instrumentation leads out of the pressure vessel.

Data Acquisition System

The data acquisition system consisted of displacement and load transducers, bridge balance unit, and recorders. The load cells used in this study were designed and built especially for this apparatus. Figure 6 shows one of the load cells used. They were instrumented to measure both axial force and torque. The strain gages, high resistance type MM EA-06-125TR-350 and EA-06-125TG-350, were carefully applied using W. T. Bean BR 610 heat curable epoxy. The bridges were connected so that the axial load and torque could be measured independently.

Total specimen deformation was measured in axial and rotational directions. Two linear infinite resolution film potentiometers mounted external to the pressure vessel were used for these measurements.

Specimen Preparation

The test specimens were cored right circular cylinders three inches in length with an inside diameter of one inch and an outside diameter of 1.5 or 1.33 inches. To ensure concentricity both core drills were mounted in one collet allowing both the inside and outside of the sample to be cored in one operation. The samples were then cut approximately to length (1.5 in.) in a diamond saw using water as a coolant and lubricant. The ends were ground to parallelness of ± .0005 inch with a diamond grinding wheel. The specimen wall thickness varied less than 0.001 inch throughout each specimen. Measured specimen dimensions were used in data reduction to eliminate the effects of specimen to specimen variations.

Testing Procedures

The samples described in the previous section were bonded into end caps with epoxy cement using an alignment jig to ensure concentricity. The samples were then jacketed both on the inside and outside by a 30 mil thick polyurethane membrane. A photograph of a sample is shown in Figure 6.

The sample and instrumentation, including load cell, were placed in the pressure vessel. The sequence of steps in running the tests was as follows: (1) the confining pressure was raised to the desired level and held constant using pressure control feedback, (2) the axial load was applied using load control feedback, and (3) the shear stress was applied. A function generator was used to apply a constant torsional displacement rate.

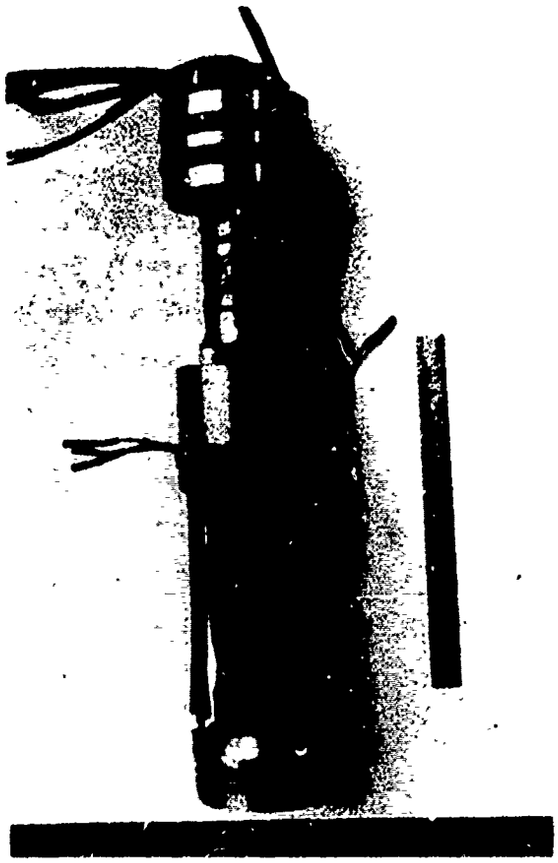

Figure 6. Torsional joint specimen, load cell, and cantilever displacement gages.

The normal and tangential displacement, the axial load, and the torque were recorded on x-y recorders for the slower strain rate tests. For the higher strain rate tests the torque was recorded on an oscilloscope. At all rates the confining pressure was recorded on an Offner Dynagraph Recorder.

Description of Rock

The rock used in this study was Westerly granite, and was obtained from the Bureau of Mines Twin Cities Research Center. The rock is composed of about 1/3 quartz, 1/3 potash feldspar and 1/3 plagioclase feldspar with traces of micas and other minerals.[22] Westerly granite has a density of 2.63 gm/cm^3, a grain size of 0.8 - 1.2 mm and a porosity of 0.007 by volume. The static unconfined compression strength is 37 ksi.[21]

Variation in Shear Stress Across Specimen Wall

As was stated previously a major disadvantage in using hollow cylindrical samples is that the shear stress varies across the specimen wall. According to the linear theory of elasticity the shear stress τ increases linearly with radius r as described by the equation

$$\tau = \frac{Tr}{J}$$

where T is the applied torque and J is the polar moment of inertia. According to this equation the shear stress at the inside radius of the joint surface would be between 25 and 33 percent lower than that at the outside radius. However, the effect of joint slip greatly modifies the stress distribution and must be taken into account. This can be seen by considering an idealization of joint deformation. The simplest case would be if the slip stress were constant, independent of joint slip displacement. For this ideal case the joint characteristics are similar to those of a perfectly plastic material and the resulting stress distribution would be the same, i.e. constant shear stress across the joint of the torsion specimen. Thus it may be concluded that once slip occurs the stress distribution across the joint in the hollow torsion specimen is more nearly uniform.

The slip stress of real rock joints depends on the slip displacement. Since the slip displacement also varies across the joint, the stress

distribution for a real rock will not be exactly uniform. For smooth joint slip this effect is much less than indicated by the elastic stress gradient and is probably on the order of a few percent at most. For stick-slip deformation the situation is not as clear, since large changes in shear stress can occur with joint displacement. The variation in stress across the specimen wall during the "stick" portion of the displacement probably corresponds to that predicted by elastic theory. The details of the stress distribution as slip takes place are not clear, however. The assumption of uniform stress across the wall at slip was used for this case also, but the justification for this is much less certain than for smooth slip deformation. The uncertainty in the stress probably is bounded by elastic theory, which would be on the order of ± 12 percent.

EXPERIMENTAL RESULTS

Tests on tubular jointed specimens were carried out at several normal stresses (consisting of the hydrostatic confining pressure and the superimposed axial stress). Normal and shear stress along with both normal and tangential displacement were measured for all tests by methods described previously. The joint surfaces were all ground to a roughness of approximately 90 micro inches. The state of stress was treated as an experimental variable and the effect of loading rate was also investigated to a limited degree. The ground joint surfaces were in general modified during joint slip. A typical example is shown in Figure 7. Although the tests at the higher normal stresses showed more surface roughening during slip, a systematic investigation of the effect of the test variables on joint surface modification was not carried out.

The normal stress across the joint is the sum of the superimposed axial stress and the hydrostatic confining pressure. The shear stress was calculated from the equation

$$T \int_{R_i}^{R_o} r\tau dA$$

where T is the torque, τ is the shear stress, R_o is the outside radius, R_i is the inside radius, and dA is increment of area around the hollow cylinder. From the argument presented previously on stress gradients it was assumed that the shear stress was constant over the joint surface after slip occurred. Integrating the above equation gives

$$\tau = \frac{1.5T}{\pi(R_o^3 - R_i^3)}$$

Figure 8 shows the effect of normal stress on the maximum shearing stress for ground surfaces of Westerly granite. The data are listed in Table I. The values reported in this and other figures are the maximum value of stress obtained during a test. This value was obtained after a

Figure 7. Typical joint surface before and after testing.

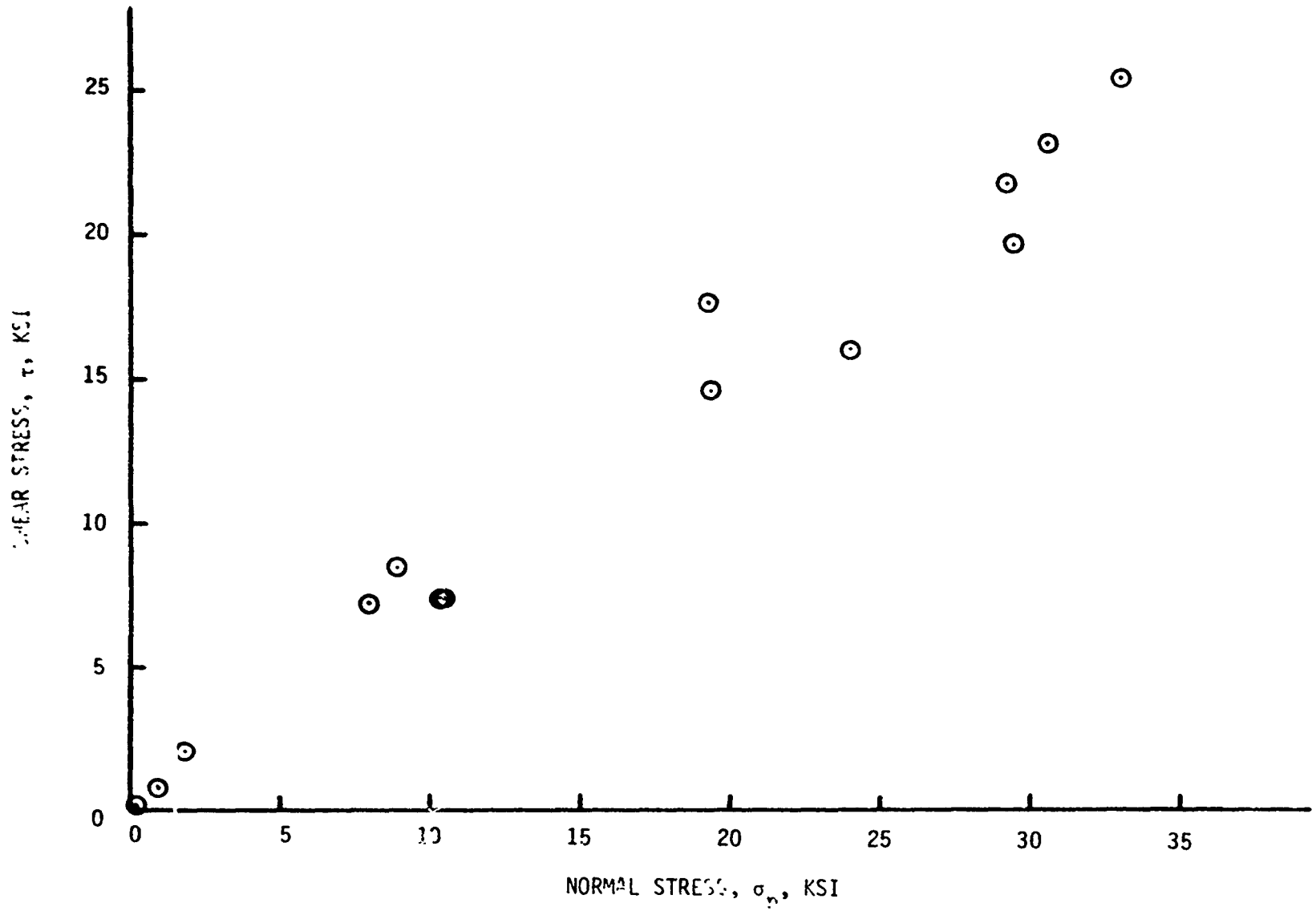

Figure 8. Effect of normal stress on maximum residual frictional shear stress for hollow cylinders of Westerly granite with ground surfaces.

TABLE I

Residual Friction Test Data

Westerly granite tested at 10^{-3} in/sec shearing displacement rate

Sample No.	Pressure (ksi)	σ_n(ksi)	τ(ksi)	μ	Comments
4-1	0	1.12	.859	.767	Stable sliding
6-2	9.93	10.5	7.31	.696	stable sliding and stick slip
7-1	6.0	8.93	8.43	.944	stable sliding and stick slip
7-2	10.1	10.4	7.45	.71	small stick slip
10-1	27.88	29.4	19.62	.667	stick slip
12-1	10.38	19.25	17.57	.912	stick slip
12-2	18.77	19.37	14.56	.752	stick slip
14-1	0	1.87	2.02	1.08	stable sliding
15-1-1	24.04	29.22	21.71	.743	stick slip
15-1-2	24.04	24.04	16.02	.666	stick slip
15-2-1	23.4	30.56	23.06	.755	stick slip
15-2-2	23.4	33.0	25.3	.767	stick slip
15-3	6.0	8.0	7.25	.91	stable sliding and small stick slip
17-1	0	.263	.119	.45	stable sliding

relatively large displacement (0.1 - 0.2 inch) and will be termed "residual shear stress" or "residual coefficient of friction." The shear stress then either remained essentially constant or dropped off slightly with increased displacement. The coefficient of friction is plotted in Figure 9 as a function of normal stress for the same tests shown in Figure 8. The coefficient of friction μ is defined as

$$\mu = \frac{\tau}{\sigma_n}$$

The variation in the data due to varying stress conditions at a given normal stress seems to be quite significant. However, when two tests were conducted at the same stress conditions the scatter was extremely small. The explanation for this will be given in the discussion section.

Figures 10-12 show plots of shear stress versus tangential joint displacement for the ground surfaces. The joint displacement was actually measured as a rotation. To convert to linear displacement the rotation in radians was multiplied by a suitable radius. This radius $\bar{r}$ was calculated from the equation

$$\bar{r} = \frac{1}{A} \int_{R_i}^{R_o} r dA$$

where A is the sample area and other variables and constants are as previously defined. Solving this equation gives

$$\bar{r} = \frac{2}{3} \frac{R_o^3 - R_i^3}{A}$$

The rotations used for calculating tangential joint displacement were measured at the ends of the specimen and thus include the torsional deformation of the intact rock as well as the joint displacement. The intact rock deformation was calculated and subtracted from the total rotation to give the corrected rotation of the joint alone. The calculation of the specimen deformation was based on linear elastic theory and the assumption of no variation in stress along the length of the specimen. A shear modulus equal to 3.4×10^6 psi was used, as given in Reference 21.

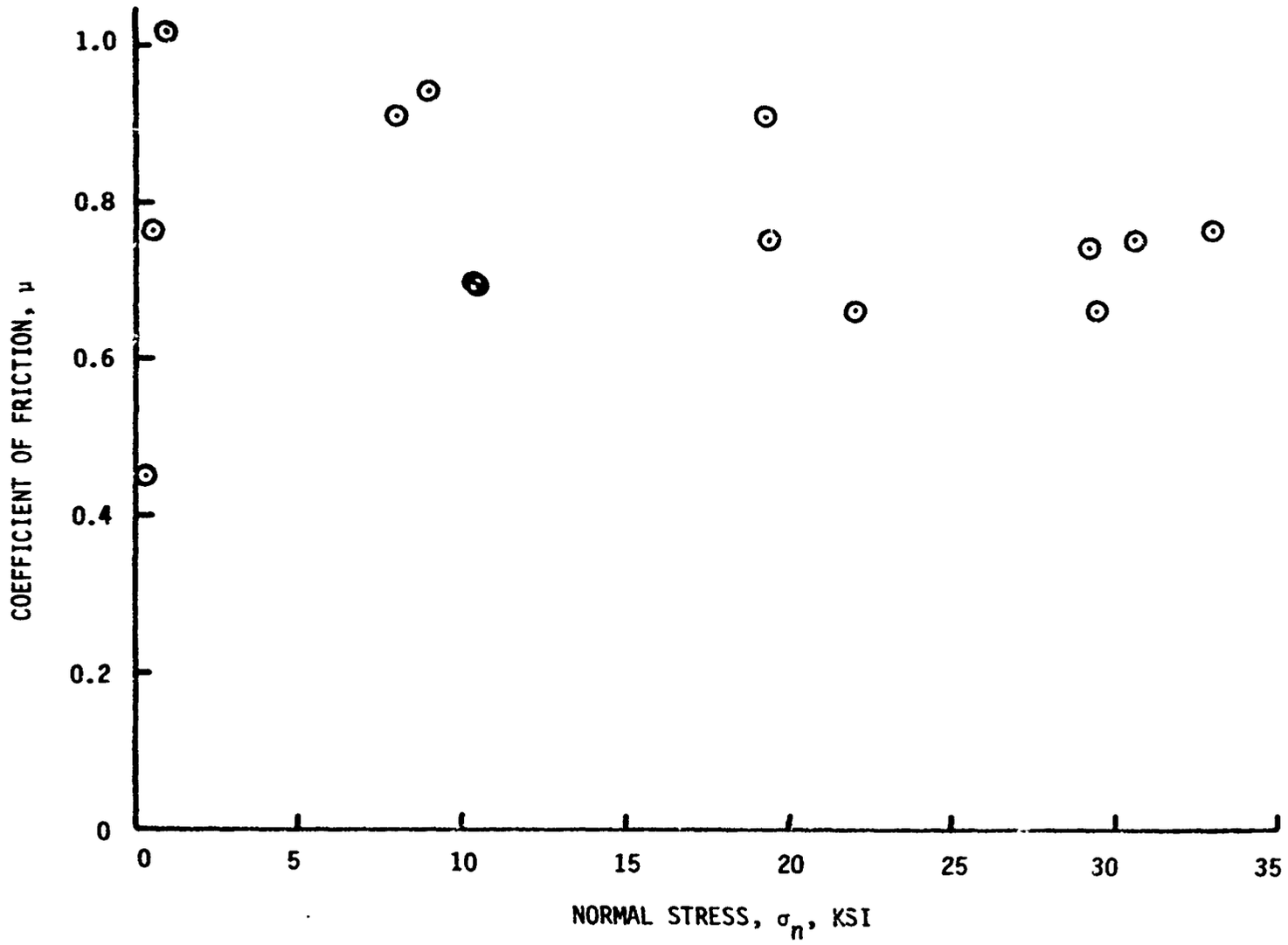

Figure 9. Effect of normal stress on residual coefficient of friction for Westerly granite with ground surfaces.

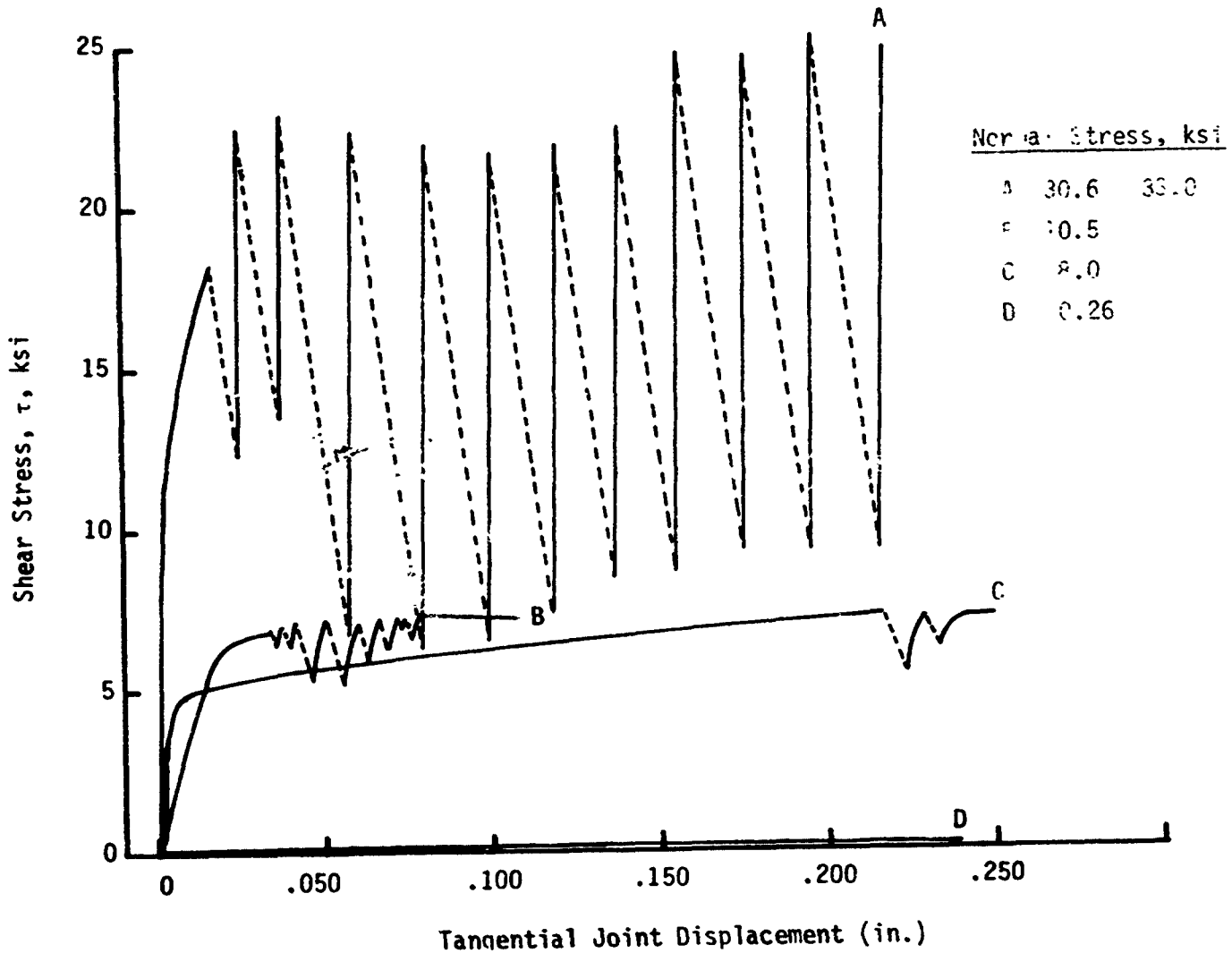

Figure 10. Effect of tangential joint displacement on shear stress for Westerly granite.

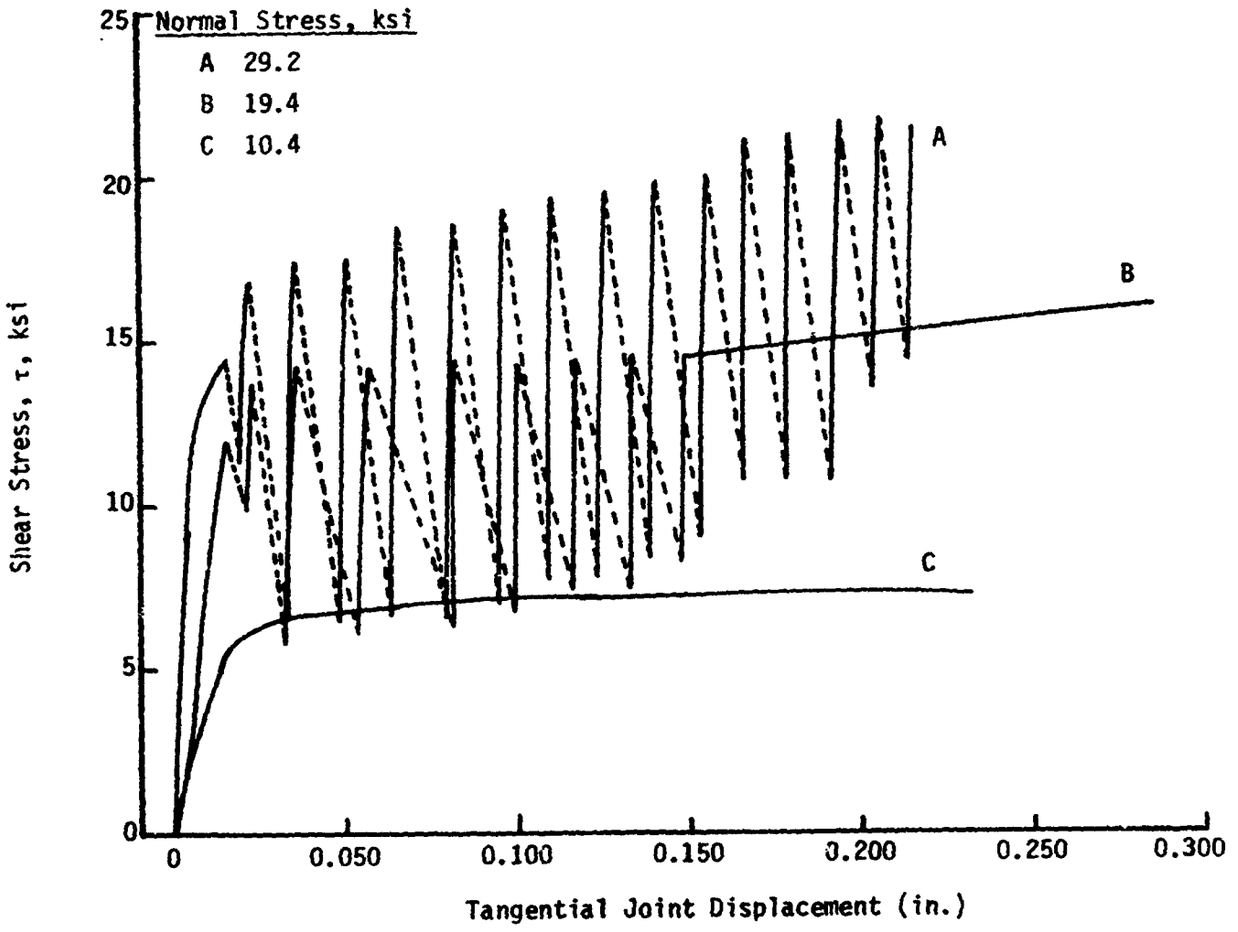

Figure 11. Effect of tangential joint displacement on shear stress for Westerly granite.

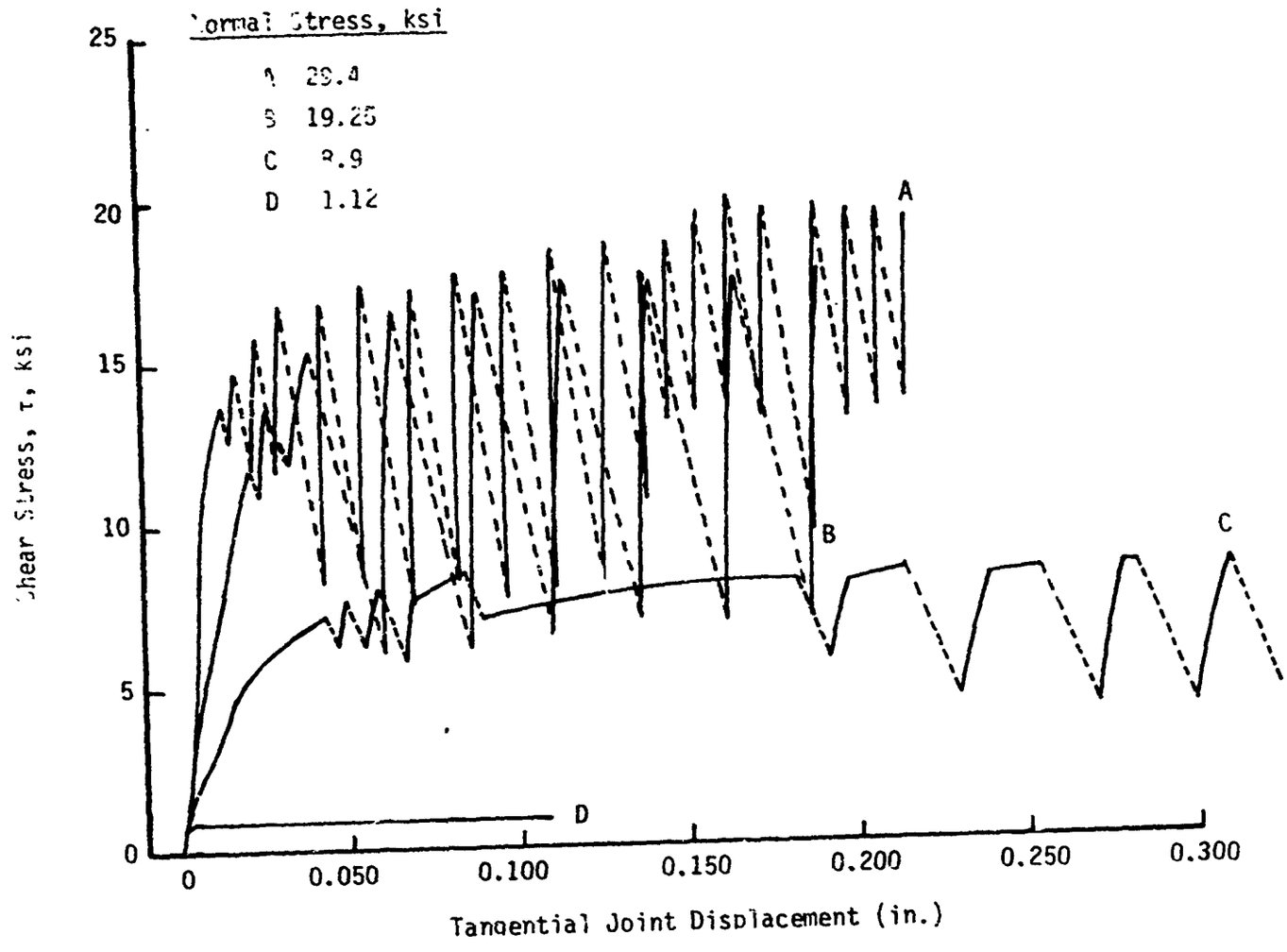

Figure 12. Effect of tangential joint displacement on shear stress for Westerly granite.

As can be seen from Figures 10-12 large stick-slip was present at higher normal stress (above 10 ksi) but not as prevalent at lower normal stress. The joint normal displacement was also measured during the shearing of the joint but for the ground surfaces the displacements were so small that the resolution of the instrumentation was inadequate.

The joint motion shown in Figures 10-12 indicates that a small joint displacement took place before the joint slipped. The stiffness of the joint appears to increase with increasing normal stress.

Rate of Deformation Test Results

Figure 13 shows the effect of deformation rate on the coefficient of friction for samples tested under equivalent state of stress before application of the shear stress. The data are also tabulated in Table II. As can be seen the increase in strain rate seems to have very little effect on the coefficient of friction. It should be noted that some of the points shown in Figure 13 have been adjusted slightly to correspond to the normal stresses shown. These changes were made according to trends established for the effect of normal stress on coefficient of friction.

Figure 14 shows plots of shear stress as a function of tangential joint displacement for the 0.1 in/sec deformation rate. Also shown is one of the tests at 0.001 in/sec deformation rate for comparison (shown in Figure 11). It can be seen that the increase in strain rate apparently has little effect on the deformation response within data scatter.

Figure 15 shows oscilloscope traces of the shear stress-time response of two of the tests carried out at the highest deformation rate, i.e. one in/sec. Since the deformation rate was approximately constant, the curves can be interpreted as shear stress vs. shearing displacement. It can be seen that stick-slip is still pronounced for the test at 20 ksi normal stress.

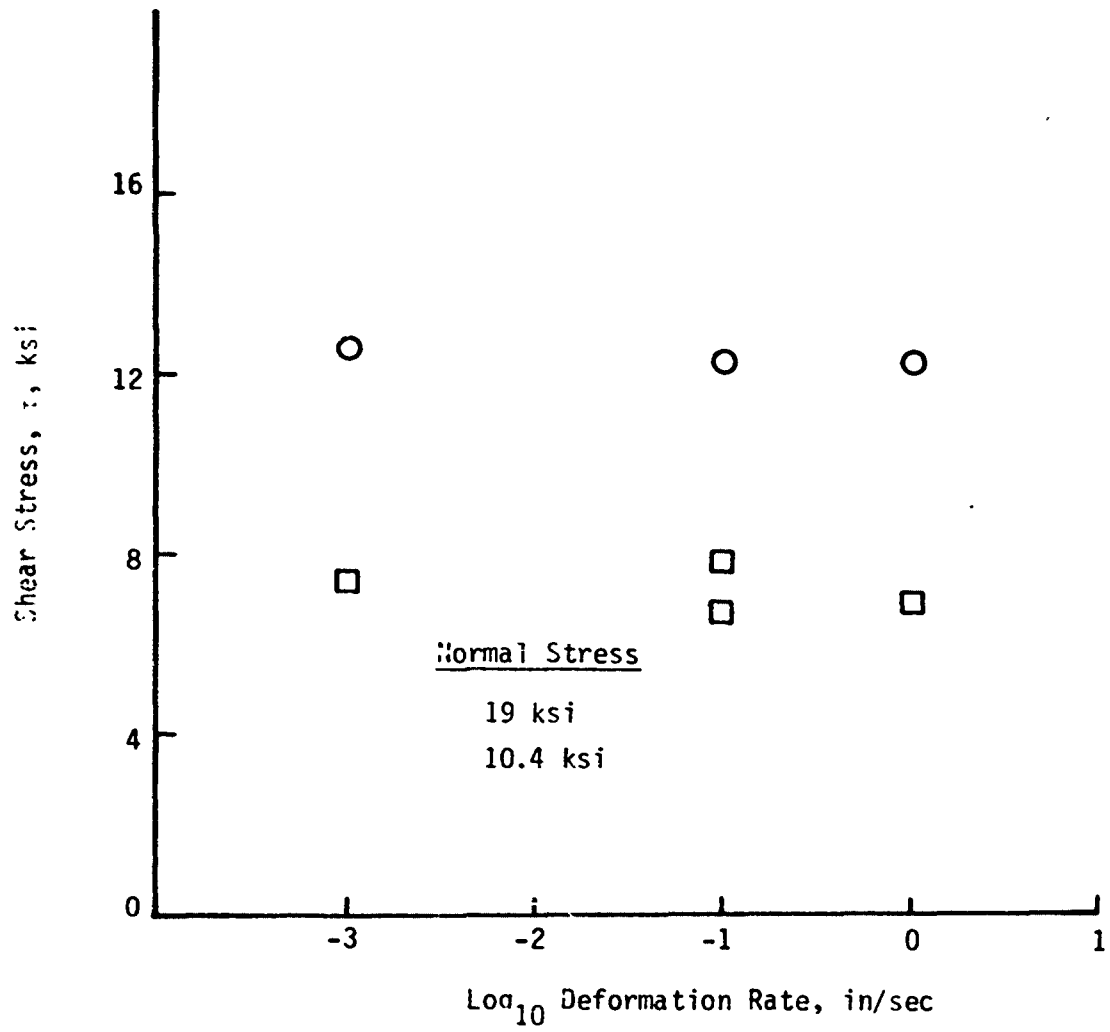

Figure 13. Effect of deformation rate on maximum shear stress for Westerly granite.

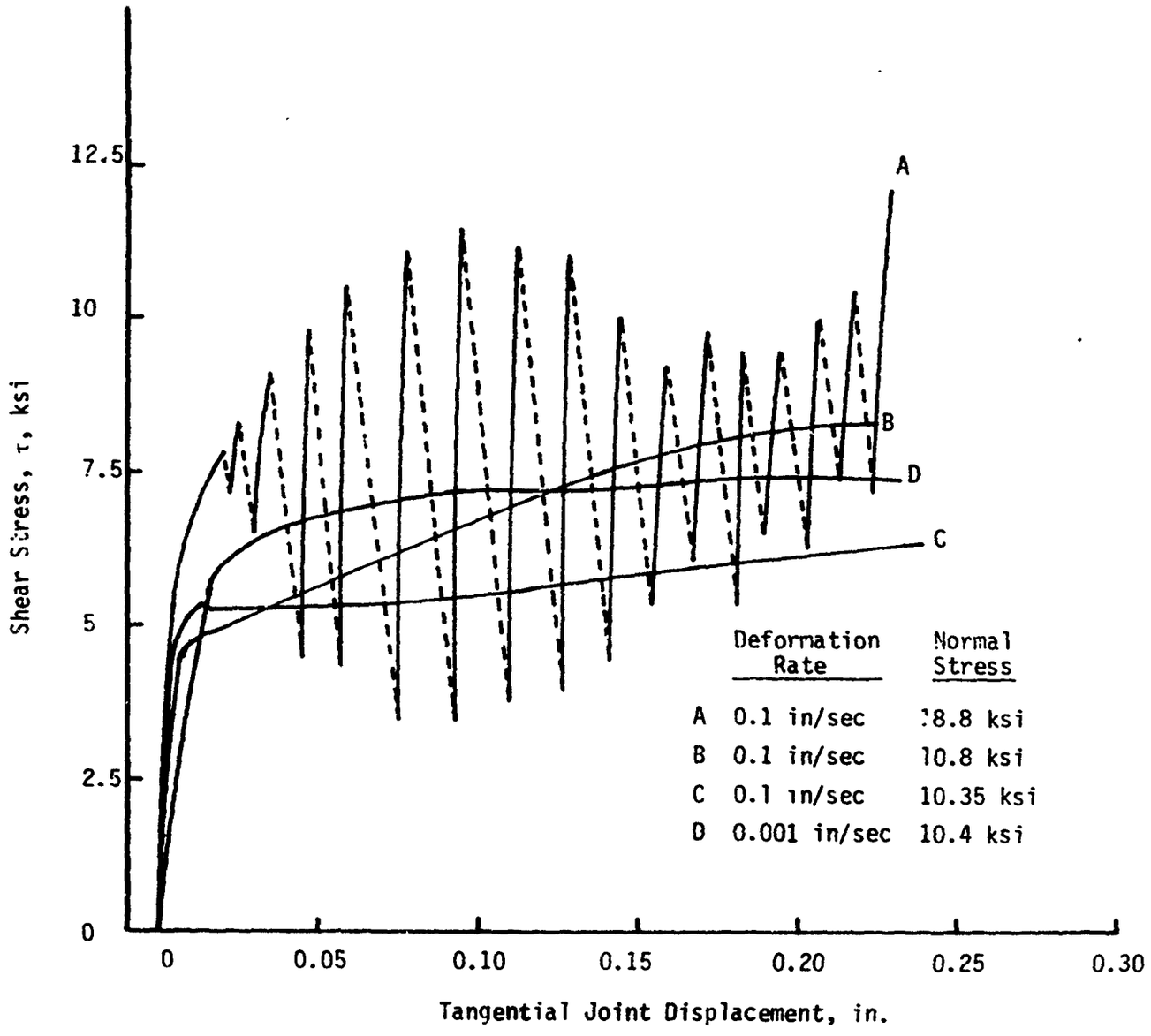

Figure 14. Shear stress versus tangential joint displacement for Westerly granite with ground friction surface at medium deformation rate.

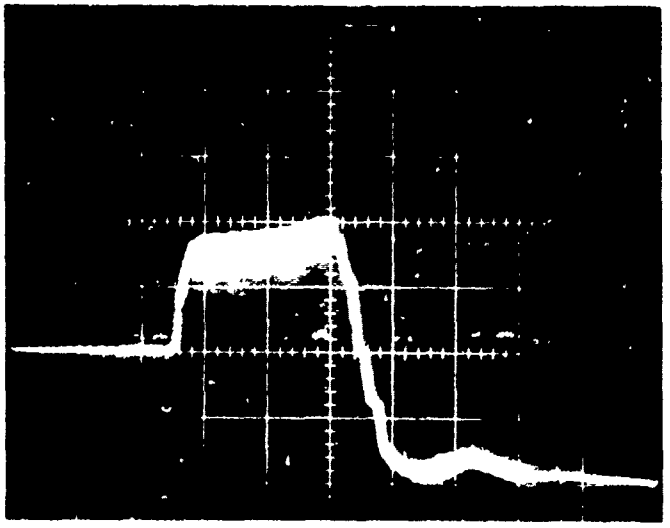

Time, 0.1 sec/cm $_n$ = 10.1 ksi

Reproduced from best available copy.

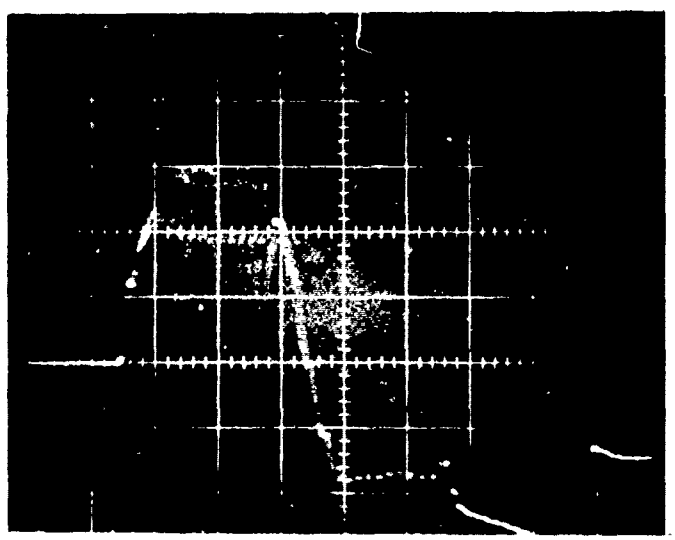

Time, 0.1 sec/cm $_n$ = 19.3

Figure 15. Oscilloscope traces for 1 in/sec deformation rate tests.

TABLE II

Medium Deformation Rate Residual Friction Test Data

Sample No.	Rate (in/sec)	Pressure (ksi)	σ_n(ksi)	τ (ksi)	μ	Comments
12-3	0.1	10.1	10.8	8.29	.768	small stick slip
16-1	0.1	16.3	18.8	12.1	.644	stick slip
16-2	0.1	10.0	10.35	6.38	.616	small stick slip
16-3	1.0	10.1	10.1	6.8	.68	small stick slip
16-4	1.0	19.3	19.3	12.4	.64	stick slip

DISCUSSION OF RESULTS

The results presented in this report can be grouped into two categories. These are: (1) the effect of state of stress on the coefficient of friction and, (2) the effect of changes in deformation rate on the joint properties. These two areas will be discussed below.

Effect of Stress on Friction

The tests at the lowest deformation rate (0.001 in/sec) were conducted with various values of joint normal stress, and in addition various values of stress parallel to the joint. It should be noted that for the torsion test the axial stress could be increased above the level of the hydrostatic pressure. In the torsion specimen the joint lateral stress is equal to the hydrostatic pressure, while the joint normal stress is equal to the hydrostatic pressure plus the superimposed axial stress. Thus due to the apparatus and specimen configuration it was possible to change the stress state of the specimen, i.e. for any given normal stress the stress state of the rock could be changed by adjusting the percentages of superimposed axial stress and hydrostatic confining pressure, which sum to the normal stress. The results shown in Figures 8 and 9 indicate that tests run at identical stress conditions showed very little scatter but changes in the state of stress apparently affected the coefficient of friction. Since the state of stress was varied widely during the study, investigation to see if this was the cause of the apparent scatter was initiated.

One of the major factors that determines characteristics such as microcracking and related stress-strain behavior in brittle rock is how close the stress is to that required for fracture. For example, Brace et al [23] have shown that microcracking starts in Westerly granite at about one-half to two-thirds of the fracture stress in triaxial compression tests. The possibility that the frictional characteristics of joints may be affected in a similar way was therefore investigated.

The concept of nearness to fracture in stress space necessarily requires a description of the fracture stress locus. It is well known that in detail the intermediate principal stress does have an effect on rock fracture, and in the present experiments on joint friction it is one of the test variable since it is equal to the joint lateral stress. Accordingly a more accurate fracture criteria was used that attempted to incorporate the intermediate principal stress effect.

A criterion was chosen from previous work of Swanson,[24], following the ideas of Mogi[25] that represents rock fracture in the following special coordinates: $\sqrt{J_2'}$ vs. $\sigma_1 + 0.1\sigma_2 + \sigma_3$, where σ_1, σ_2 and σ_3 are principal stresses and $\sqrt{J_2'}$ is the second deviatoric stress invariant given by

$$\sqrt{J_2'} = \left\{ \frac{(\sigma_{11}-\sigma_{22})^2 + (\sigma_{22}-\sigma_{33})^2 + (\sigma_{33}-\sigma_{11})^2}{6} + \sigma_{12}^2+\sigma_{23}^2+\sigma_{31}^2 \right\}^{\frac{1}{2}}$$

A plot of extension, compressio' , and biaxial fracture stress data for Westerly granite is shown plotted in these coordinates in Figure 16. The close spacing of these points indicates that a unique fracture locus is at least approximated.

The maximum joint stresses are compared with the fracture locus for intact Westerly granite in Figure 17. It can be seen that a wide difference exists among the various jointed tests in terms of how close to fracture the jointed specimens were. In fact, a number of jointed specimens did fail before slip occurred, depending on the stress conditions established for the test. These latter tests are not shown, however.

A simple criterion for nearness to fracture was defined as shown in Figure 18. As shown in this figure the "fracture coefficient" is defined as the ratio of the state of stress at residual slip to the fracture state of stress of the intact rock. The fracture coefficient is given by

$$C_f = \frac{A}{A + B}$$

where C_f is the fracture coefficient , A is the value of the second deviatoric stress invariant $\sqrt{J_2'}$ calculated for the state of stress at the joint, and A + B is the value of $\sqrt{J_2'}$ at fracture for intact rock as defined in Figure 18. The fracture coefficient is thus a measure of how close the rock at the joint was to fracture, ignoring local discontinuities in stress due to the joint.

The calculated fracture coefficient values are listed by the data points in a coefficient of friction versus normal stress plot shown in Figure 19. As can be seen a systematic variation in the coefficient of friction exists that appears to be related to the fracture coefficient.

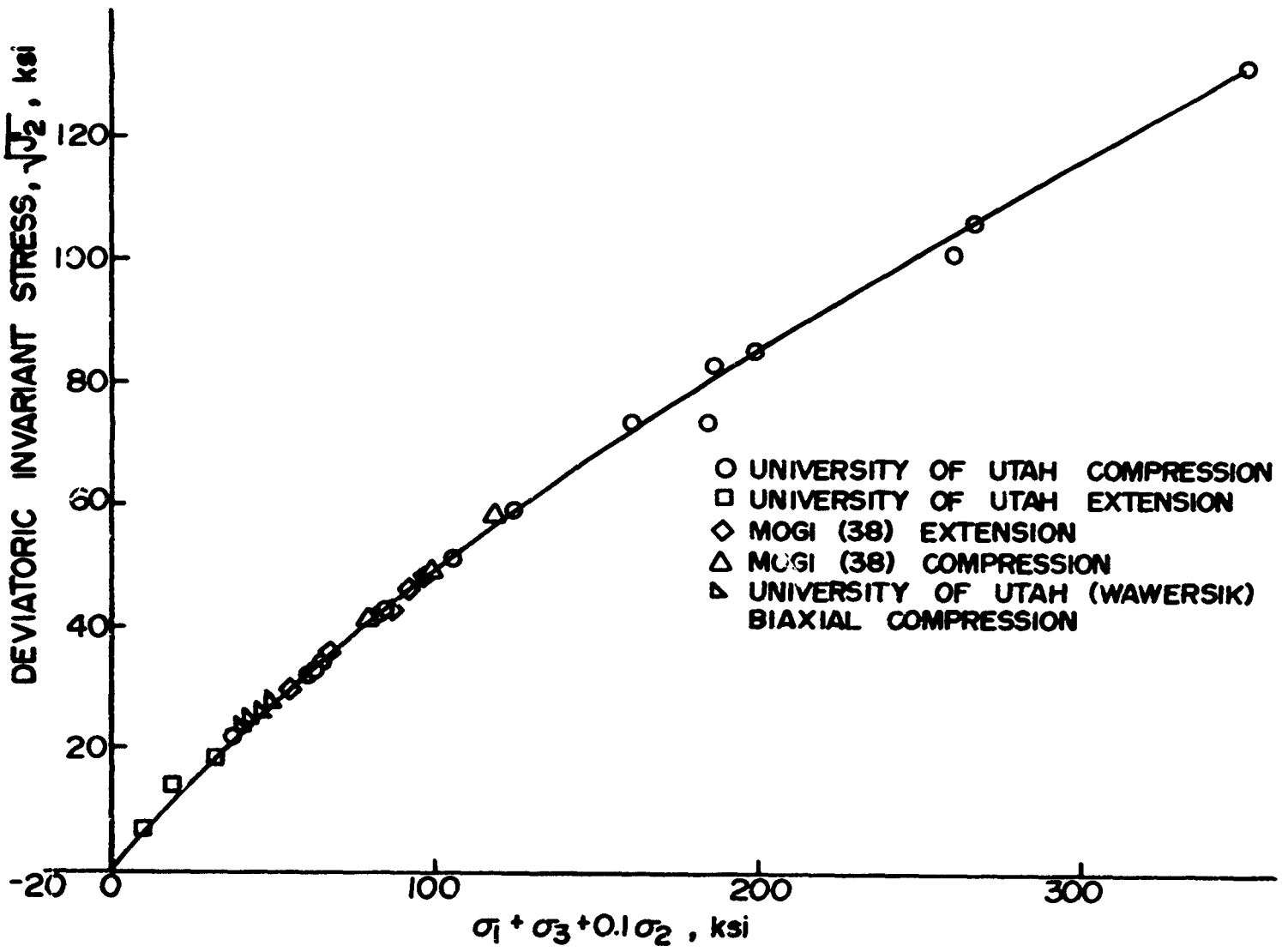

Figure 16. Failure locus for Westerly granite.

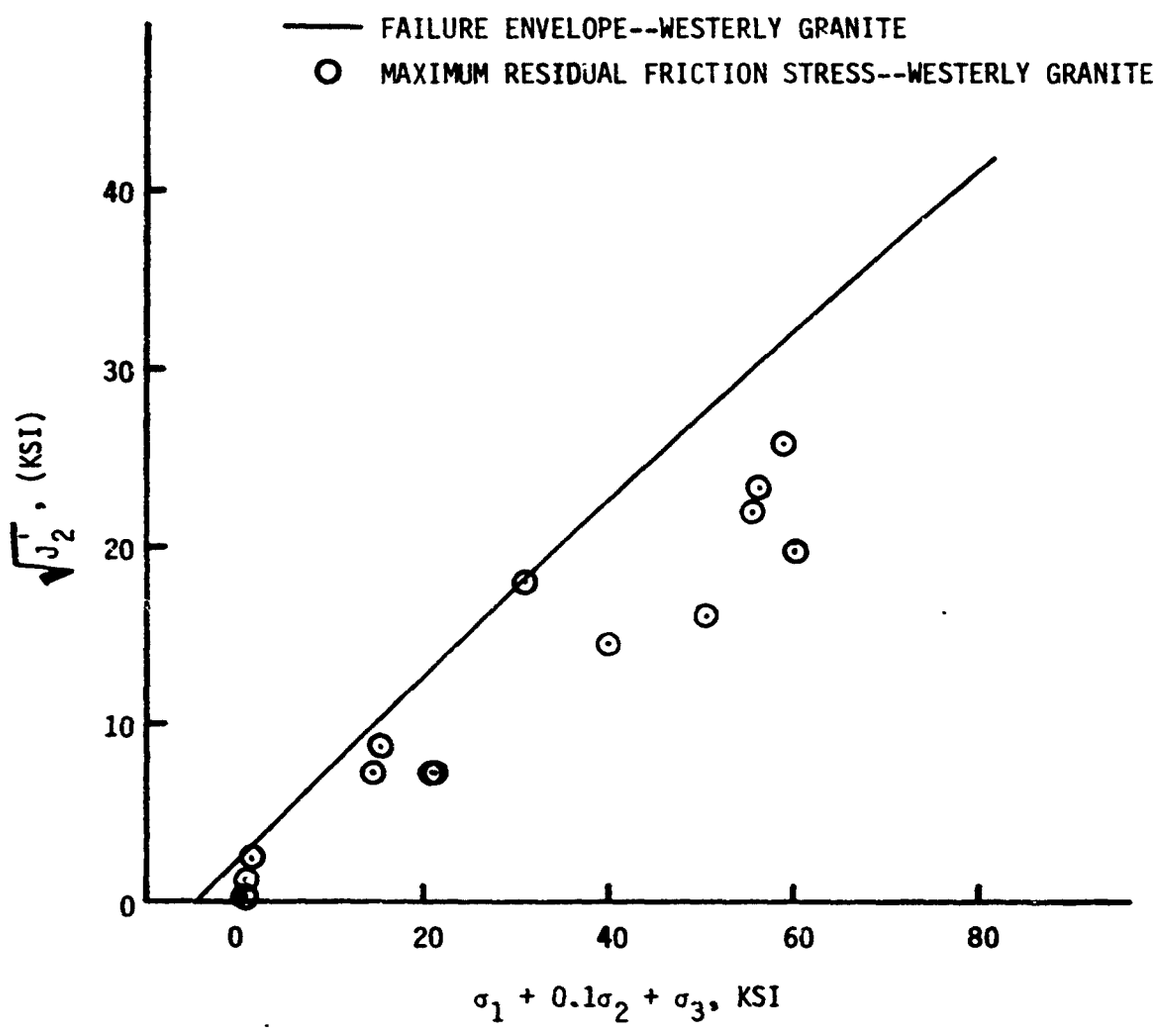

Figure 17. Comparison of failure envelope for intact rock and stress at residual slip of jointed specimens.

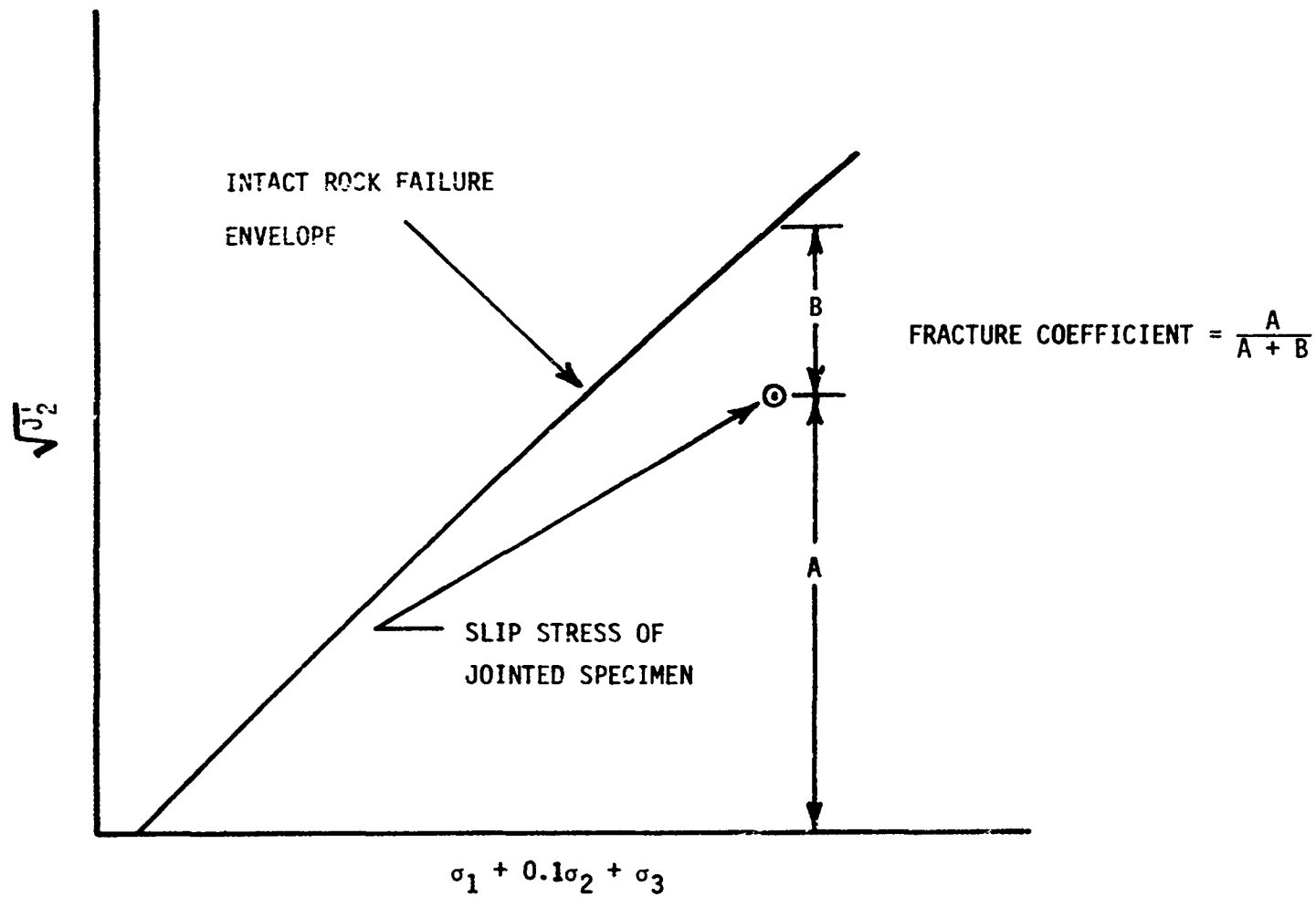

Figure 18. Illustration of calculation of fracture coefficient for jointed specimens.

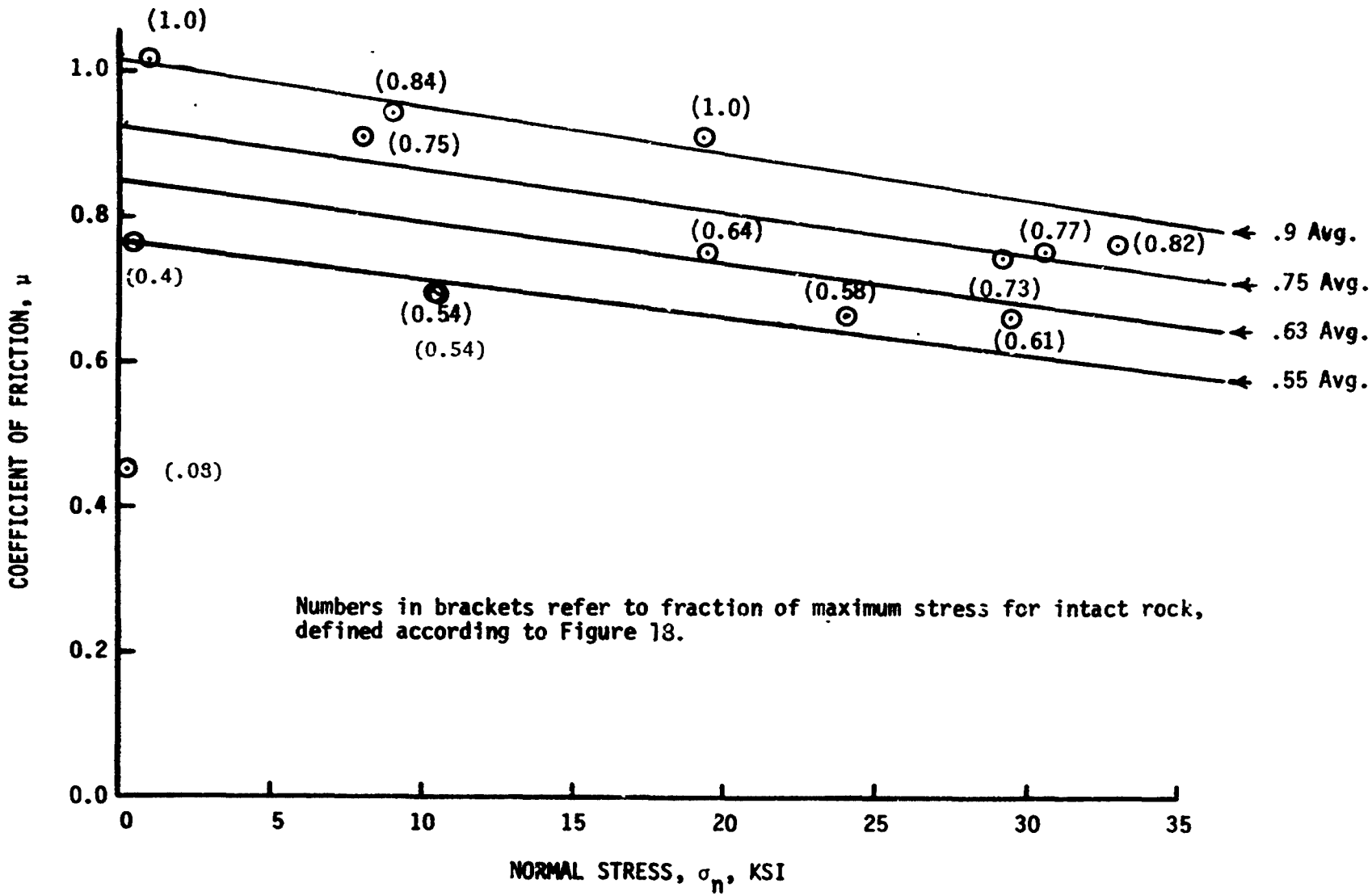

Figure 19. Effect of stress state and normal stress on residual friction for Westerly granite.

From this result, then, the variation in coefficient of friction at a given normal stress is judged to be a systematic function of the state of stress. Further this state of stress can apparently be described by the fracture coefficient described above.

The data and interpretation just given may explain some of the inconsistencies encountered previously in rock friction studies. For example, tests under triaxial compression using specimens with a given joint angle often show a decrease in coefficient of friction with increasing normal stress. However, in direct shear tests this trend may be the same or an opposite effect may be observed. This can be explained as follows. For the triaxial test with one joint angle the fracture coefficient varies only slightly over the usual range of normal stresses, as for example in Byerlee's data[11]. Thus, the coefficient of friction would be expected to decrease with normal stress according to the trends shown in Figure 19. In the direct shear tests, however, the fracture coefficient is increasing with increased normal stress. For example, increasing the normal stress from 500 to 1000 psi would be expected to increase the fracture coefficient of Westerly granite on the order of 80%. Therefore, the coefficient of friction could increase, decrease or stay the same depending on how the fracture coefficient increases with normal stress and how the coefficient of friction decreases with normal stress.

A comparison with Byerlee's data[11] on ground surfaces in triaxial tests with joint angles of 45^{0} is shown in Figure 20. Although Byerlee's data is at higher normal stresses than the present study, the general trends of the data can be compared. It can be seen that the higher coefficients of friction obtained from the torsion data appear to correlate with Byerlee's data, but as discussed previously much variation is seen in the torsion data.

It is interesting to consider the effect of the state of stress on this comparison. A calculation of the fracture coefficient for Byerlee's data shows that the slip stresses in 45^{0} jointed triaxial tests will be very close to 0.9 over the full range of Byerlee's data. If only the data from the torsion tests that correspond to a fracture coefficient of 0.9 are compared, good agreement, as shown in Figure 21, is obtained. In this case a

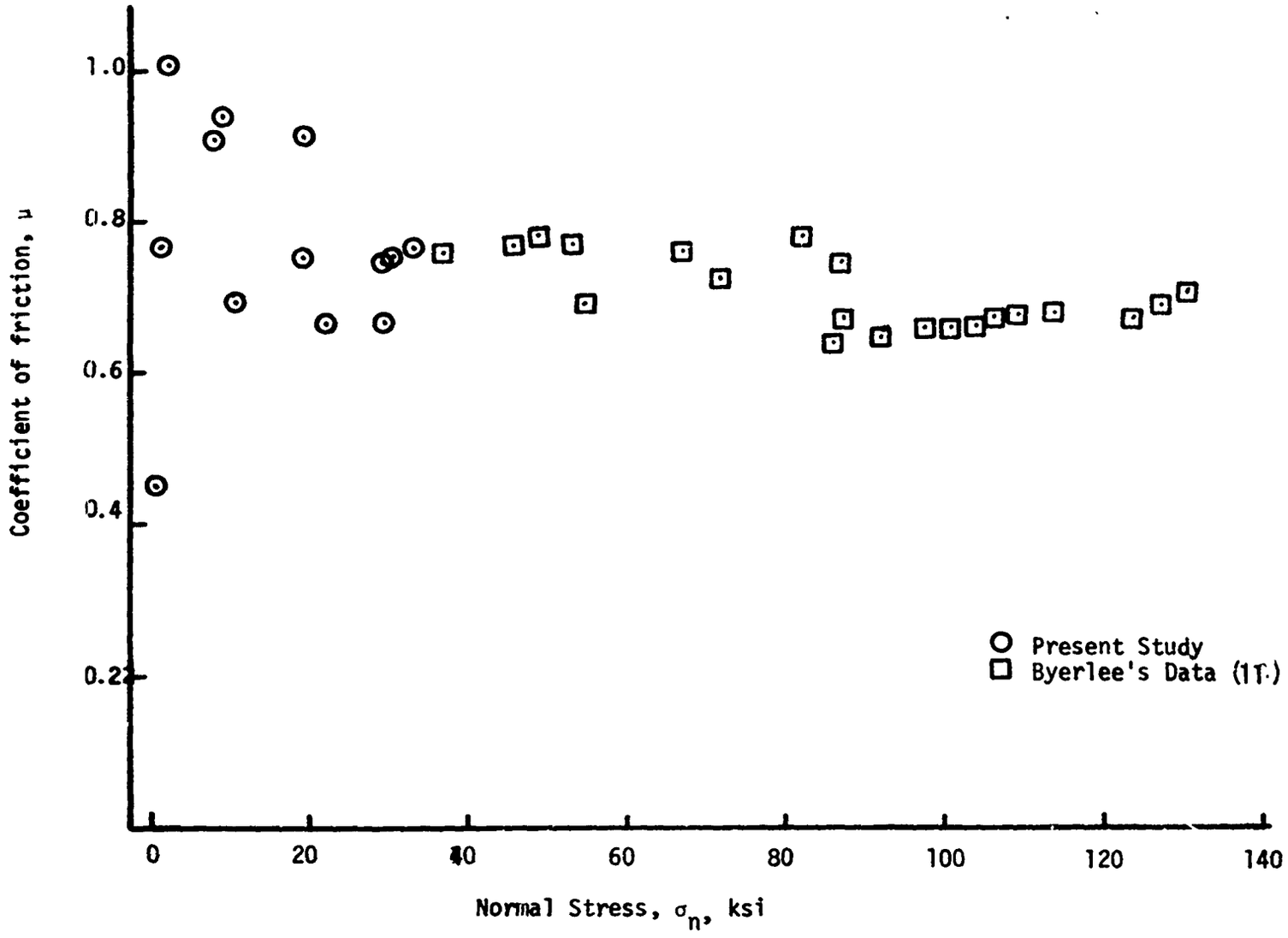

Figure 20. Comparison of present data with Byerlee's data for Westerly granite.

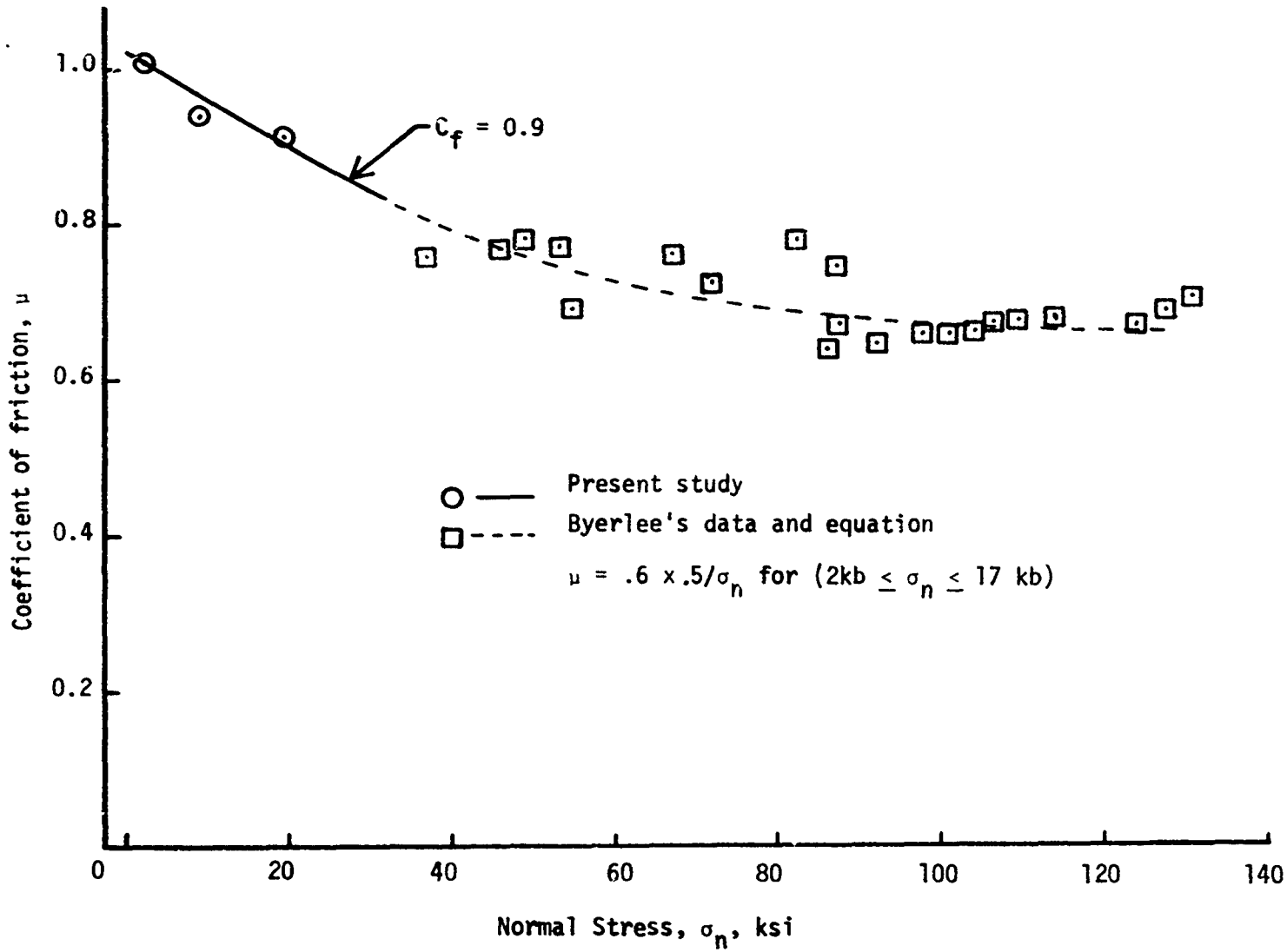

Figure 21. Comparison of present data and theory with Byerlee's data of Westerly granite.

much better comparison appears to hold, and the effect of normal stress on the coefficient of friction is established over a wide range of normal stress.

It has been suggested by Byerlee[11] that the frictional results of triaxial tests do not depend on the joint angle. Since the state of stress in the specimen does depend on the joint angle (as the ratio of confining pressure to normal stress varies) this would seem to be at variance with the present results. For example, the fracture coefficient for a 30 degree triaxial joint is close to 0.76 for Westerly granite, as compared to 0.9 for the 45 degree joint. The difference that this would make on the shear stress, as calculated from Figure 19, is shown in Figure 22. It can be seen that the difference in the shear stress between 30 and 45 degree joints predicted by the present theory is not large and could easily be masked by data scatter. The dashed line represents Byerlee's equation for coefficient of friction given by

$$\mu = .6 + 0.5\sigma_n \text{ for } (2 \text{ kb} < \sigma < 17 \text{ kb})$$

Rate of Deformation Effects

The results shown in Figure 13 indicate little change in the maximum shear stress with shearing deformation rate over the range 0.001 to 1 in/sec. This appears to be somewhat surprising in view of the rate dependence of the compressive strength of Westerly granite established previously (22, 26).

It appears from comparing these results with the rate dependency observed by Dieterich[8] that the loading effect rate effect on normal stress may be different than the effect on shear stress. In the present study the time of application of the normal stress was held constant, and only the shearing rate was varied.

It has been suggested [15, 16] that stick-slip joint motion would not occur at high loading rates. The oscilloscope traces shown in Figure 15 do not support this view, at least for rate of 1 in/sec. The stick-slip motion is clearly revealed by the apparent "ringing" of the shear stress record.

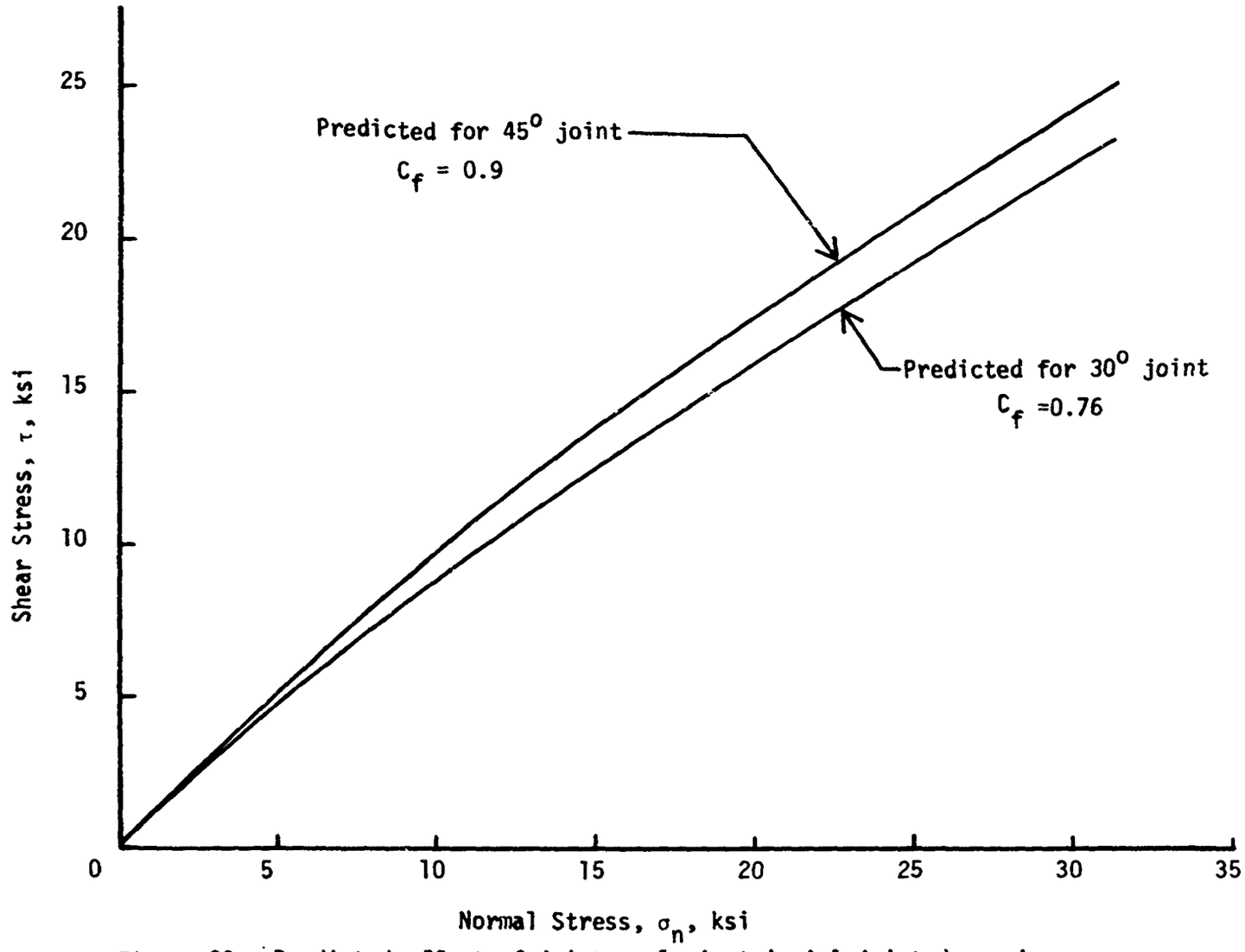

Figure 22. Predicted effect of joint angle in triaxial jointed specimen.

SUMMARY AND CONCLUSIONS

A laboratory investigation of the strength and deformation of jointed tubular samples of Westerly granite with ground (90 micro inch) surfaces has been completed. Special attention was given to the effect of varying the state of stress on the joint. This was accomplished by varying the lateral stress on the joint and the normal stress on the joint independently.

The following conclusions are drawn from the investigation:

1. Torsional shear loading of a tubular specimen is advantageous for joint friction studies in several respects. For example, normal stress can be varied over a wide range, large deformations can be applied and the general state of stress can be varied. Also both normal and tangential joint displacements can be conveniently measured.
2. The state of stress has a definite effect on joint frictional properties. This effect was correlated well by a parameter that describes the nearness of the stress state to fracture of the competent rock.
3. The mode of deformation at low normal stresses is stable sliding while at high normal stresses the mode is stick-slip. The transition takes place at approximately a normal stress of 10 ksi. This value may vary slightly with both deformation rate and state of stress.
4. The stiffness of the joint before slip and during stick-slip increases with increasing normal stress.
5. The effect of shearing deformation rate on residual joint friction was small and showed essentially no change within data scatter for a three decade change in rate of loading.
6. At rates of deformation to 1 in/sec stick-slip was still the mode of deformation at higher normal stresses.

ACKNOWLEDGMENT

This work was sponsored by the Defense Nuclear Agency through Terra Tek, Inc. contract DNA001-73-C-0034. The authors acknowledge the thoughtful suggestions of the contract technical monitors, Mr. S. J. Green of Terra Tek, Inc. and Mr. C. B. McFarland of the Defense Nuclear Agency. Bryan Smith was very helpful in assisting with the experiments.

REFERENCES

1. Jaeger, J. S., and Cook, N. G. W., "Fundamentals of Rock Mechanics." Methuen, 1969.

2. Coulson, J. H., "The Effects of Surface Roughness on the Shear Strength of Joints in Rocks," Tech. Report MRD-2-70, Missouri River Div. Corps of Eng., 1970.

3. Pratt, H. R., Black, A. D., and Bonney, F. J., "Frictional Properties of Cedar City Quartz Diorite," Tech. Report AFWL-TR-72-122, Kirtland Air Force Base, New Mexico, 1972.

4. Patton, F. D., "Multiple Modes of Shear Failure in Rock and Related Materials," Ph.D. Thesis Department of Geology, University of Illinois, 1966.

5. Hoskins, E. R., Jaeger, J. C., and Rosengren, K. J., "A Medium Scale Direct Friction Experiment," Int. J. Rock Mech. and Min. Sci., 5, (143-154) 1968.

6. Maurer, W. C., "Shear Failure of Rock Under Compression," J. Soc. of Petroleum Eng., 5, 2 (167-176) 1965.

7. Byerlee, J. D., "Theory of Friction Based on Brittle Fracture," J. Appl. Phy., 38, 7 (2928-2934) 1967.

8. Dieterich, J. H., "Time Dependent Friction in Rocks," J. Geophy. Res., 77, 20 (3690-3697) 1972.

9. Jaeger, J. C., and Cook, N. G. W., "Friction in Granular Materials," Structure Solid Mechanics and Engineering Design. Proceedings Southampton 1969 Civil Eng. Matl. Conf., ed. M. Te eni, Wiley-Interscience, 1971, pp. 257-266.

10. Jaeger, J. C., and Rosengren, K. J., "Friction and Sliding of Joints," Proc. Austin Inst. Min. Met. No. 229, 1969.

11. Byerlee, J. D., "Frictional Characteristics of Granite under High Confining Pressure," J. Geophy. Res., 72, 14 (3639-3648) 1967.

12. Byerlee, J. D., "Brittle-Ductile Transition in Rocks," J. Geophy. Res., 73, 14 (4741-4750) 1968.

13. Brown, W. S., and Swanson, S. R., "Laboratory Study of Rock Joint Strength and Stiffnesses under Confining Pressure," Univ. of Utah Final Report, No. F29601-71-C-0050, Kirtland Air Force Base, New Mexico, 1972.

14. Brace, W. F., and Byerlee, J. D., "Stick-Slip as a Mechanism for Earthquakes," Science, 153, (990-992) 1966.

15. Byerlee, J. D., and Brace, W. F., "Stick-Slip Stable Sliding, and Earthquakes - Effect of Rock Type, Pressure, Strain Rate and Stiffness," J. Geophys. Res., 73, 18 (6031-6037) 1968.

16. Byerlee, J. D., "Static and Kinetic Friction of Granite at Higher Normal Stress," Int. J. Rock Mech. and Min. Sci., 7, (557-582) 1970.

17. Bowden, F. P., and Tabor, D., The Friction and Lubrication of Solids, Vol. 2, Clarendon Oxford, 1964, p. 79.

18. Rabinowicz, E., Friction and Wear of Materials, John Wiley: New York, 1965, pp. 97-99.

19. Dokos, S. J., "Sliding Friction under Extreme Pressure," J. Appl. Mech., 13, (A148-A156) 1946.

20. Kutter, H. K., "Stress Distribution in Direct Shear Test Samples," Proceedings of the International Symposium, ISRM, Nancy, France, 1971.

21. Brown, W. S., and Swanson, S. R., "Constitutive Equations for Westerly Granite and Cedar City Tonalite for a Variety of Loading Conditions," Univ. of Utah Final Report DASA-2473, March, 1970.

22. Green, S. J., and Perkins, R. D., "Uniaxial Compression Tests at Strain Rates from 10^{-4} to 10^{4}/sec on Three Geologic Materials," Final Report DASA-2199, January, 1969, p. 49. Also presented at the 10th Symposium on Rock Mechanics, Austin, Texas, 1968.

23. Brace, W. F., Paulding, B. W., and Scholz, C., "Dilatancy in the Fracture of Crystalline Rocks," J. Geophys. Res., 71, (3939-3953) 1966.

24. Swanson, S. R., unpublished work, University of Utah, 1972.

25. Mogi, K., "Fracture and Flow of Rocks under High Triaxial Compression," J. Geophys. Res., 76, (1255-1269) 1971.

26. Brown, W. S., Swanson, S. R., and Wawersik, W. R., "Further Studies of Dynamic and Biaxial Loading of Rock," Univ. of Utah Final Report DNA 28871, February, 1972.